

# THE KINEMATIC CONNECTION BETWEEN QSO-ABSORBING GAS AND GALAXIES AT INTERMEDIATE REDSHIFT <sup>1,2</sup>

CHARLES C. STEIDEL<sup>3</sup>, JUNA A. KOLLMEIER<sup>4</sup>, AND ALICE E. SHAPLEY

*Palomar Observatory, California Institute of Technology, MS 105-24, Pasadena, CA 91125*

CHRISTOPHER W. CHURCHILL

*Pennsylvania State University, Department of Astronomy and Astrophysics, 525 Davey Lab,  
University Park, PA 16802*

MARK DICKINSON

*Space Telescope Science Institute, 3700 San Martin Drive, Baltimore, MD 21218*

MAX PETTINI

*Institute of Astronomy, Madingley Road, Cambridge CB3 0HA, UK*

## ABSTRACT

We present complementary data on 5 intermediate redshift ( $0.44 \leq z \leq 0.66$ ) Mg II absorbing galaxies, combining high spatial resolution imaging from *Hubble Space Telescope*, high-resolution QSO spectroscopy from Keck/HIRES, and galaxy kinematics from intermediate resolution spectroscopy using Keck/LRIS. These data allow a direct comparison of the kinematics of gas at large galactocentric impact parameters with the galaxy kinematics obtained from the faint galaxy spectroscopy. All 5 galaxies appear to be relatively normal spirals, with measured rotation curves yielding circular velocities in the range  $100 \leq v_c \leq 260 \text{ km s}^{-1}$ . The QSO sightlines have projected impact parameters to the absorbing galaxies in the range  $14.5h^{-1} \leq d \leq 75h^{-1} \text{ kpc}$ ; the galaxies have inclination angles with respect to the line of sight ranging from 40 to 75 deg. We find that in 4 of the 5 cases examined, the velocities of all of the Mg II absorption components lie entirely to one side of the galaxy systemic redshift. The fifth case, for which

---

<sup>1</sup>Based, in part, on data obtained at the W.M. Keck Observatory, which is operated as a scientific partnership among the California Institute of Technology, the University of California, and NASA, and was made possible by the generous financial support of the W.M. Keck Foundation.

<sup>2</sup>Based, in part, on data obtained with the NASA/ESA Hubble Space Telescope, which is operated by the Space Telescope Science Institute for the Associated Universities for Research in Astronomy, Inc., under NASA contract NAS5-26555.

<sup>3</sup>Packard Fellow

<sup>4</sup>Present address: Ohio State University, Department of Astronomy

the galaxy is much less luminous than the other 4, has narrow absorption centered at zero velocity with respect to systemic despite having the largest disk inclination angle in the sample. These observations are consistent with rotation being dominant for the absorbing gas kinematics; however, the total *range* of velocities observed is inconsistent with simple disk rotation in every case. Simple kinematic models that simultaneously explain both the systemic offset of the absorbing material relative to the galaxy redshifts, *and* the total velocity width spanned by the absorption, require either extremely thick rotating gas layers, rotation velocities that vary with  $z$  height above the extrapolation of the galactic plane, or both. In any case, our small sample suggests that rotating “halo” gas is a common feature of intermediate redshift spiral galaxies, and that the kinematic signature of rotation dominates over radial infall or outflow even for gas well away from the galactic plane. We discuss possible explanations for this behavior, and compare our observations to possible local analogs.

*Subject headings:* galaxies:distances and redshifts–galaxies: halos – galaxies:evolution–galaxies:kinematics and dynamics– quasars: absorption lines

## 1. INTRODUCTION

Metallic absorption lines in the spectra of background QSOs and the nature of their association with galaxies have been subjects of considerable interest over the last decade. A number of circumstantial pieces of evidence, accumulated during the first  $\sim 20$  years of QSO absorption line research, pointed to galaxies as being responsible: e.g. the tendency for systems to split into complexes of total velocity extent consistent with galaxy-sized potential wells, the presence of metals which were presumably produced *in situ*, and clustering properties that resembled that of galaxies. However, exploring the details of the connection between absorption systems and galaxies did not become possible until later work began to directly identify galaxies responsible for individual QSO absorption line systems (Bergeron & Boissé 1991; Steidel, Dickinson,& Persson 1994 (SDP); Le Brun et al. 1997). This connection is extremely interesting in the context of our understanding of galaxy evolution and galactic structure because QSO absorption line systems have the potential to explore the gas-phase physical conditions, geometry, and kinematics of galaxies with what can be many orders of magnitude increased sensitivity compared to direct observations of the galaxies. Moreover, the sensitivity of absorption line measurements is largely independent of galaxy redshift, and thus provides the opportunity to study the evolution, over very large time baselines, of characteristics that can be much more subtle than those accessible using traditional faint galaxy techniques.

At present, most identification of absorption systems with individual galaxies is tenuous at best. If a faint galaxy is found near the line of sight with a redshift in agreement with the measured redshift of the QSO absorption system, it is generally taken as a positive identification of the actual

object producing the absorption. This type of statistical approach has been adopted by most studies of intermediate redshift metallic absorption systems (e.g., BB91; SDP; Le Brun et al. 1997). There are very few cases where relatively exhaustive spectroscopy down to faint magnitude limits has been obtained for all objects within several hundred kpc of the QSO line of sight (cf. Steidel et al. 1997), making the identifications of each absorber more secure. Possible selection effects inherent in this type of identification procedure have been outlined by Charlton & Churchill (1996).

The state of knowledge of the types of galaxies producing various classes of QSO absorption systems varies considerably as a function of redshift and of absorption system taxonomy. The most work has been done at  $z \lesssim 1$ , for absorption line systems selected by the presence of Mg II  $\lambda\lambda 2796, 2803$  doublets with absorption line rest-frame equivalent widths  $W_\lambda > 0.3 \text{ \AA}$  (BB91; SDP, Steidel 1995). These relatively strong Mg II-selected systems are generally associated with gas having  $N(\text{H I}) \gtrsim 10^{17} \text{ cm}^{-2}$  (i.e., “Lyman limit systems”), and so would be expected to probe (on average) the outer parts of galaxies where the H I is more highly ionized than disk gas observed for nearby galaxies. The galaxies responsible for the Mg II absorption at intermediate redshift ( $\langle z \rangle \simeq 0.6$ ), statistically, appear to be drawn from normal field galaxies with luminosities within  $\sim 1.5$  magnitude of present-day  $L^*$  (BB91; SDP94). More recent morphological studies using *HST*, of which the data in this paper are a subset, have shown that the identified galaxies are generally of relatively normal morphologies identifiable along the Hubble sequence (Dickinson & Steidel 1996; Steidel 1998, Steidel et al. 1997). The colors and magnitudes of these galaxies appear to exhibit little or no evolution with redshift over the range  $0.3 \lesssim z \lesssim 0.9$ , in agreement with general studies of field galaxy evolution (e.g., SDP, Lilly et al. 1996; Vogt et al. 1996). There is some evidence that the observed distribution of “impact parameters”, the projected physical distance between the putative absorbing galaxy and the QSO sightline at the galaxy redshift, is consistent with a roughly spherical distribution of gas of radius  $R(L)$  that is a weak function of luminosity (SDP, Steidel 1995, 1998):

$$R(L_K) \simeq 38h^{-1} \text{kpc} \left( \frac{L_K}{L_K^*} \right)^{0.2} .$$

A flattened disk-like geometry is not as favored by the existing statistics, but any geometry in which the gas layer has finite thickness compared to its radial extent is very difficult to rule out with present statistics on impact parameters and the incidence of interlopers (cf. Charlton & Churchill 1996). Given the available statistics, however, and the likely stochastic nature of the sizes and shapes of gaseous envelopes around field galaxies, simple geometric pictures should be viewed as no more than working models.

Damped Lyman  $\alpha$  systems, which are metal line systems for which  $N(\text{HI}) \geq 2 \times 10^{20} \text{ cm}^{-2}$  (cf. Wolfe et al. 1986), have also received a great deal of attention in the context of what their kinematics can tell us about galaxies, particularly at high redshift. In a series of papers, Prochaska & Wolfe (1997,1998) present analyses of the kinematics of high redshift damped Lyman  $\alpha$  systems ( $z \gtrsim 2$ ), concluding that the “edge leading asymmetry” often seen in the velocity profiles of DLAs is most consistent with rotating thick disks with  $v_c \gtrsim 200 \text{ km s}^{-1}$ . Other work has claimed that

the kinematics can be explained by aggregates of small galactic fragments as would naturally be present in hierarchical structure formation models (Haehnelt, Steinmetz, & Rauch 1998) or simply from randomly moving clouds in spherical halos (McDonald & Miralda-Escudé 1999), although all models appear to have problems reproducing the relative velocities of the low-ionization and high ionization species in the damped Lyman  $\alpha$  systems (Wolfe & Prochaska 2000). At present, little or no information on the galaxies themselves is available at these high redshifts, so that the disk inclination angles, impact parameters, and galaxy systemic redshifts are generally unknown. At lower redshifts, in contrast to the Mg II absorbers, both ground-based and HST observations of the galaxies indicate that the galaxies associated with the high column density absorbers are a very “mixed bag”, ranging from dwarf galaxies as faint as  $0.05 L^*$  to normal spirals (Steidel et al. 1994; Steidel et al. 1997; Le Brun et al. 1997; Turnshek et al. 2000; Bowen, Tripp, & Jenkins 2001). In many cases spectroscopy of the putative DLA absorbers has been difficult or impossible because of the very small impact parameters (and resulting problems with scattered light from the QSOs) that often obtain for DLAs. It should be emphasized that every DLA is also a Mg II system (cf. Rao & Turnshek 2000), but that the Mg II systems are sensitive to gas with H I column densities up to  $\sim 3$  orders of magnitude smaller than that which will produce a DLA. It is certainly possible that disk-like kinematics could dominate many Mg II systems even when the impact parameter is well beyond the  $10^{20} \text{ cm}^{-2}$  H I contour. In any case, studies of systems where the absorption line kinematics and the galaxy properties can be used simultaneously to constrain kinematic models would be very valuable for understanding the DLA systems at high redshift. For the moment, this can only be done at substantially lower redshifts ( $z \lesssim 1$ ).

The advent of echelle spectrographs on 8m-class telescopes has allowed relatively routine high dispersion spectroscopy of the same QSOs that have been used historically for Mg II absorption surveys (e.g., Steidel & Sargent 1992). There has been a fair amount of activity in examining the kinematics of the intermediate redshift Mg II systems (to scales as fine as  $\sim 5 \text{ km s}^{-1}$ ) and comparing them with what is known about the absorbing galaxy photometric properties and the observed impact parameters (Lanzetta & Bowen 1992; Churchill, Steidel, & Vogt 1996; Churchill & Vogt 2001). The relatively small samples of absorption system/absorbing galaxy pairs studied so far do not provide any obvious clues to the nature of absorbing gas in relation to the galaxies, or at least no strong systematic trends. So far, the issues of the geometry, physical conditions, and kinematics of the absorbing gas have not been considered in concert with simultaneous access to high quality imaging and spectroscopic data on the faint galaxy absorbing candidates. And yet, it is now possible with 8m-class telescopes to obtain spectra of quality sufficient to trace the kinematics of galaxy rotation curves to  $z \sim 1$  (e.g., Vogt et al. 1996), and it is clearly straightforward to obtain high quality images with kpc-scale resolution for galaxies in the same redshift range using *Hubble Space Telescope* (HST).

In this paper, we present pilot observations that provide first results and explore the feasibility of establishing directly the kinematic connection between gas at large galactocentric impact parameters, and the luminous component of the galaxies. At the very least, it should be possible to

test the hypothesis that the absorbing gas is dynamically associated with the identified absorbing galaxy using greatly improved redshift and kinematic measurements of both the absorbing gas and the luminous material in the galaxy. At best, we hope to establish the nature of the absorbing gas; some possibilities include:

- The gas is an extension of the galaxy disk, and the kinematics of the absorbing material are entirely compatible with a kinematic extension of the observed galaxy rotation curve. If this is the case, there may be an opportunity for measuring galaxy rotation curves out to much larger galactocentric radii than is normally possible, particularly for galaxies at relatively high redshift.
- The velocities of the galaxy and the absorption are too discrepant for the gas to be plausibly associated with the identified galaxy; the true absorber may remain unidentified.
- The galaxy and gas-phase kinematics exhibit the same general kinematic spread and zero net offset, as might be expected if the absorbing gas takes the form of distributed “clouds” or substructure with random velocities relative to systemic
- Some combination of the above.

The paper is organized as follows. In §2 we present the data. §3 contains a general discussion of results in each of the 5 fields, and §4 explores simple kinematic models to explain the observations. Finally, in §5 we discuss the general results and their implications.

## 2. DATA

The QSO/absorbing galaxy fields observed in this pilot program were chosen from among the 25 fields of intermediate redshift Mg II–selected absorption line systems we observed with *Hubble Space Telescope*. All of these QSO fields have been included in existing analyses of the statistics of Mg II absorbing galaxies (e.g., Steidel, Dickinson, & Persson 1994) and most were observed as part of a large low-resolution survey for  $0.2 \leq z \leq 2.2$  Mg II absorption systems (Steidel & Sargent 1992). More details are given in §3.

The initial targets for this project were *not* chosen at random from among the Mg II absorbing galaxies at redshifts where [OII]  $\lambda 3727$  would be accessible at optical wavelengths. Rather, they were chosen to have apparent brightnesses and morphologies that would allow for interesting galaxy kinematics. Most of them have large inclination angles with respect to the line of sight, and all but 1 are brighter than  $\mathcal{R}=22$ , so that very high quality spectra could be obtained without large investments in observing time. Choosing galaxies with relatively large inclination angles also (in principle) allows extending kinematic measurements of the galaxy rotation curves well beyond the luminous portions using the absorption line kinematics, which should be sensitive to H I column densities perhaps 100 times smaller than most 21-cm measurements of galaxies in the local universe.

While it is generally the case that the galaxies identified as Mg II absorbers at intermediate redshifts are classifiable along the full range of the Hubble sequence (Steidel 1998), in the case of the 5 galaxies in this pilot sample, all appear morphologically to be normal mid-to-late-type spiral galaxies, albeit at redshifts of  $\sim 0.5$ . All but one are close to present-day  $L^*$  in rest-frame blue luminosity (see Table 1).

## 2.1. Ground-based Imaging

Optical and near-IR photometry of the galaxies of interest was available from ground-based observations obtained primarily during the years 1991-94 as part of a more extensive survey of Mg II absorbing galaxies (Steidel, Dickinson, & Persson 1994). The data for the 5 fields discussed in this paper were obtained using the Kitt Peak National Observatory 2.1m telescope (optical) and 4m Mayall telescope (near-IR). Some of the relevant data are collected in Table 1. The optical  $\mathcal{R}$  passband, through which all of the fields were observed, has an effective wavelength of 6930 Å and thus is a very close approximation to rest-frame B at a redshift of  $z = 0.5 - 0.6$ . The  $\mathcal{R}$  magnitudes were converted to rest-frame B absolute magnitudes using k-corrections appropriate to the best-fit spectral type from the optical and optical/IR colors. These k-corrections were in all cases smaller than 0.2 mag. With the exception of G1 1222+228, which has a luminosity of only  $\sim 0.25L^*$ , all of the galaxies are comparable to or more luminous than the present-day  $L^*$  of  $M_B \simeq -19.5$  (Folkes et al. 1999; Blanton et al. 2001).

Spectroscopic confirmation of the absorbing galaxies in this sample had been obtained previously for G1 1038+064 (Bergeron & Boissé 1991), and for the other galaxies through our own spectroscopic efforts using the Lick Observatory Shane 3m telescope in the 1991-93 observing seasons. The spectroscopic identifications of G1 1222+228 and G1 1317+276 were both tentative due to poor-quality spectra; as discussed in §3 below, the Keck spectroscopy led to substantial revisions of the absorbing galaxy situation in those two cases.

Also listed in Table 1 are the angular separation of the galaxies from the QSO, in arc seconds, and the projected impact parameter in  $h^{-1}$  kpc.

## 2.2. HST Imaging

Images of each of the QSO fields discussed in this paper were obtained using WFPC-2 during Cycles 5 and 6 as part of a more general HST imaging survey of QSO absorbing galaxies at intermediate redshifts. The details of the observations are summarized in Table 2. In brief, each field was observed in the F702W filter (again, in order to be well-matched to rest-frame B at the typical absorber redshift of  $z_{abs} \simeq 0.6$ , and for compatibility with our existing ground-based data discussed above) for two orbits, with standard CR-split exposures during each orbit and a non-integral pixel dither between orbits to allow for partial recovery of the spatial resolution that is

degraded by under-sampling. The images were reduced using the “variable pixel linear combination” (or “drizzling”) technique (Fruchter & Hook 1997) onto a final pixel scale of  $0''.05 \text{ pixel}^{-1}$ . In each case, the QSO was centered on the Wide Field Camera chip 3; portions of the reduced images, with the galaxies of interest marked, are shown in Figures 1-5. Galaxy inclination angles  $\theta_i$  with respect to the plane of the sky, resulting from fits to the galaxy isophotes, are given in Table 2.

### 2.3. Galaxy Spectroscopy

Spectra of the absorbing galaxies were obtained in 1999 March using LRIS (Oke et al. 1995) on the Keck II telescope. As detailed in Table 3, 3 of the galaxy spectra were obtained with a  $1''.0$  long slit. The position angle of the slit was chosen to lie along the major axis of the galaxy of interest (in the case of G1 Q1222+228), to include 2 galaxies near the QSO sightline in the case where there was ambiguity about the identification of the absorber (as for G1,G2 Q1317+2743), or in order to minimize to leakage of scattered QSO light into the slit (as for Q1148+3842). For the two other cases (G1 Q0827+2421 and G1 Q1038+0625) the observations were obtained through a slit mask (also having 1.0 arc sec slitlets) whose position angle was chosen so that the slit of primary interest lay along the major axis of the absorbing galaxy. A 600 line/mm grating blazed at  $7500 \text{ \AA}$  and tilted so as to place redshifted [OII]  $\lambda 3727$  emission near the center of the spectral format, was used for all of the observations. With the 1.0 arc sec slits, the resulting spectral resolution was  $4.5 \text{ \AA}$  or  $\sim 225 \text{ km s}^{-1}$  at the wavelengths of interest for measuring [OII]  $\lambda 3727$  at  $z \simeq 0.6$ .

The data were flat-fielded using exposures of a halogen lamp internal to the spectrograph. Sky subtraction was accomplished by fitting a polynomial function to each spatial column of the spectrogram, in the usual fashion. Extended line emission was then evident for each galaxy over a spatial region of  $\sim 2$  arc seconds along the slit. We extracted individual one-dimensional spectra by co-adding 3-pixel swaths (which corresponds to approximately one resolution element of  $\simeq 0.65$  arc seconds) at one pixel (0.215 arc seconds) increments along the slit (so that adjacent spectra are not completely independent of one another). Wavelength calibration, which is crucial given our interest in an external comparison of measured velocities, was accomplished by extracting spectra of HgArNeKr arc line lamps at the same spatial pixels as the extracted galaxy spectra. In order to account for the possibility of instrumental flexure between the time the data and the arc lamps were obtained, we adjusted the wavelength solutions for each individual galaxy exposure (generally there were two exposures, each of 1200s duration, with a spatial dither along the slit in between) using night sky emission lines. The RMS residuals of the wavelength solutions were  $\sim 0.2 \text{ \AA}$ , or about  $10 \text{ km s}^{-1}$  at the wavelengths of interest. Wavelengths were reduced to heliocentric to facilitate the comparison with the absorption line kinematics.

Rotation curves were measured for each galaxy by fitting the position of the [OII] doublet at each spatial position over the extent of the galaxy, in a manner similar to that described in Vogt et al. 1996. Uncertainties in the emission line velocities were estimated from the RMS uncertainties produced by the fitting procedure; these uncertainties are typically  $25 \text{ km s}^{-1}$  per spatial point,

or about one tenth of a spectral resolution element. The systemic redshift of each galaxy was taken to be the velocity at the position of the centroid of the continuum (averaged over one spatial resolution element) on the 2-dimensional spectrogram. The resulting rotation curves are plotted for each galaxy in Figures 1-5.

Circular velocities  $v_c$  were estimated for each galaxy by assuming that the extreme observed velocity with respect to systemic is equal to  $v_c \sin \theta_1$ . These estimates must be viewed as approximate, since it is not obvious that the observed rotation curves extend far enough to have reached their asymptotic values, and because of uncertainties in  $\theta_i$ . In any case, our conclusions are not strongly affected by lack of precision in the estimates of  $v_c$ .

## 2.4. QSO Spectroscopy

Spectra of the 5 QSOs were obtained using the HIRES echelle spectrometer on the Keck I telescope (Vogt et al. 1994), all using a  $0''.85$  slit resulting in spectral resolution of  $6.6 \text{ km s}^{-1}$ . Three of the QSOs were observed in 1995 January, with the details of the observations and reductions described in Churchill & Vogt (2001). Two of the QSOs were observed in 1998 February and March, one using the blue-blazed cross-disperser (Q0827+2421). The echelle and cross-disperser angles were chosen so as to include at least the Mg II  $\lambda\lambda 2796, 2803$  doublet at the redshift of a known QSO absorbing galaxy; in most cases several other low-ionization transitions were also observed.

The 1998 HIRES data were reduced using MAKEE (T. Barlow, private communication), a package tailored to the reduction of HIRES data. The output of MAKEE is an extracted spectrum of each echelle order, corrected for the echelle blaze function, and transformed to vacuum, heliocentric velocities. A summary of the HIRES observations is provided in Table 4. Relevant portions of the HIRES spectra are shown in Figures 1-5.

## 3. Discussion of Individual Fields

### 3.1. Q0827+243 (OJ 248)

The absorption system at  $z_{abs} = 0.52499$  is among the strongest Mg II systems known, with the  $\lambda 2796$  component having a rest-frame equivalent width of  $2.47 \text{ \AA}$ . The Mg II absorption is strongly saturated, with a total velocity width of  $\simeq 270 \text{ km s}^{-1}$ ; some insight into the kinematic structure is possible by looking at the apparently unsaturated Mg I  $\lambda 2853$  line, which shows at least 4 components of roughly equal strength spread over the entire velocity range covered by the Mg II “trough”. This system is known to be a DLA (Rao & Turnshek 2000), with a measured H I column density of  $2 \times 10^{20} \text{ cm}^{-2}$  (which could include gas over the full  $\sim 300 \text{ km s}^{-1}$  velocity range).



The spectrum of the absorbing galaxy, which was obtained with the slit oriented along the major axis of the galaxy, yields a rotation curve over the velocity range  $-180 \leq v_{gal} \leq 240 \text{ km s}^{-1}$ , but the blue-shifted side of the galaxy is clearly affected by a satellite galaxy that appears to be distorting the galaxy disk and which has a systemic velocity different from the galaxy of interest (skewed toward positive velocities, as can be seen in the top panel of Figure 1b). It is unclear how or if this apparent satellite is affecting the kinematics of the absorbing gas—there is no Mg II absorption at positive velocities, but it is possible that some of the kinematic complexities of the gas may be induced by an imminent merger event. Because of this distortion to the galaxy morphology (whatever its cause), the inclination angle of the galaxy (measured to be  $i = 69^\circ$ ) is rather uncertain. Assuming this inclination angle, the galaxy rotation speed is  $v_c \simeq 260 \text{ km s}^{-1}$ , evaluated from the side of the rotation curve that is unaffected by the satellite (i.e., at positive velocities with respect to systemic). Unlike the other 4 galaxies discussed in this paper, G1 0827+243 has very strong [OII] emission ( $W_\lambda^0 \simeq 50 \text{ \AA}$ ) characteristic of vigorous current star formation. The rest-frame B luminosity of  $\sim 1.6$  times present-day  $L^*$ , may be significantly enhanced by this star formation.

The absorbing gas kinematics are qualitatively as would be expected for a model in which the extrema of the absorbing gas velocities are consistent with a kinematic extension of the disk gas seen in emission, but extending to somewhat larger velocities at an impact parameter of  $25.4h^{-1}$  kpc. We discuss more detailed kinematic models for this system in §4.1.

### 3.2. Q1038+064 (4C 06.41)

The absorption system at  $z_{abs} = 0.4415$  has been known for more than 20 years (Burbidge et al. 1977; Weymann et al. 1979) and the absorbing galaxy was among the first intermediate-redshift systems identified (Bergeron & Boisse´ 1991). The *HST* image in Figure 2a clearly shows that the absorbing galaxy is a luminous but relatively normal mid-type spiral, with an inclination angle of  $i = 60^\circ$ . The rotation curve of the galaxy is well-determined, with an observed rotational velocity of  $v_c \sin \theta_i \simeq 225 \text{ km s}^{-1}$ , or a de-projected rotation speed of  $v_c^{corr} \simeq 260 \text{ km s}^{-1}$ . The absorbing gas follows the kinematics of the emitting material nicely, indicating an extreme velocity of  $\simeq 250 \text{ km s}^{-1}$  relative to the galaxy systemic velocity, with the sign as expected for a simple extension of the rotation curve to a disk impact parameter of  $44.8h^{-1}$  kpc. If the absorbing gas is interpreted as an extension of a flat rotation curve to a galactocentric radius of  $\simeq 45h^{-1}$  kpc, the minimum implied virial mass of the galaxy is  $\simeq 7h^{-1} \times 10^{11} M_\odot$ . We discuss the kinematic model for this system in §4.2.

The Mg I  $\lambda 2853$  absorption is very weak, with only one component securely detected at  $v_{sys} = -120 \text{ km s}^{-1}$  and a marginal detection of the  $v_{sys} \simeq -180 \text{ km s}^{-1}$  component that is the strongest in Mg II. Inspection of an archival HST Faint Object Spectrograph spectrum of Q1038+064 reveals a Lyman limit system at a redshift compatible with that of the Mg II system. Assuming that the scattered light correction for the FOS spectrum is accurate, the  $z = 0.4415$  system has an optical depth at the Lyman limit of  $\tau_{LL} \simeq 1.6$ , or  $\log N(\text{H I}) \simeq 17.3$ . Thus, there is evidence

that a significant component of the extended gas giving rise to the Mg II absorption has disk-like kinematics despite the relatively low total H I column density.

### 3.3. Q1148+387 (4C 38.31)

The  $z_{abs} = 0.5531$  absorption system was first identified by Steidel & Sargent 1992 (SS92). As evident in Figure 3a, the absorbing galaxy is a mid-type spiral only moderately inclined with respect to the line of sight ( $\theta_i \simeq 40^\circ$ ), and as such the amplitude of the observed rotation curve is only  $v_c \sin \theta_i \simeq 125 \text{ km s}^{-1}$ . The (somewhat uncertain) corrected rotational velocity is  $v_c \simeq 195 \text{ km s}^{-1}$ , consistent with or slightly low given the galaxy’s luminosity. The QSO sightline, which is only  $14.4h^{-1} \text{ kpc}$  in projection from the galaxy, still apparently samples only blue-shifted gas-phase velocities. However, the kinematic extent of the gas is significantly broader than the range of velocities seen from the galaxy rotation curve, and the absorbing gas appears to be distributed into  $\sim 6$  individual velocity components, all with about the same relative strength of Mg II and Fe II  $\lambda 2600$  absorption. We discuss kinematic models for this system in §4.3.

The total H I column density of this system can be estimated from an archival FOS spectrum. Again assuming that the zero point of the FOS flux scale is accurate, the optical depth is  $\tau_{LL} \simeq 1.5$ , or  $\log N(\text{H I}) \simeq 17.2$ . This would appear to be an unexpectedly low H I column given that the impact parameter is at a projected galactocentric distance of only  $14.4h^{-1} \text{ kpc}$  (corresponding to a disk impact parameter of  $18.8h^{-1} \text{ kpc}$  given the inclination angle). Apparently either the QSO sightline has found a “hole” in the H I distribution, or the outer disk of G1 1148+387 is relatively H I-poor.

### 3.4. Q1222+228 (Ton 1530)

The originally-targeted Mg II redshift along this line of sight was the  $z_{abs} = 0.6681$  system first discovered by Young, Sargent, & Boksenberg (1982). We believed, on the basis of galaxy spectra of admittedly marginal quality, that this system was produced by the nearly-edge-on spiral which was the primary target of our LRIS spectroscopy. We were somewhat surprised to find that the galaxy instead has an emission redshift of  $z_{gal} = 0.5502$  (leaving the much stronger  $z_{abs} = 0.6681$  absorption system without a confirmed absorbing galaxy candidate) from the much-higher-quality Keck/LRIS spectra. An *a posteriori* search of the HIRES spectrum yielded a weak Mg II doublet, with  $W_0(\lambda 2796) = 0.08 \text{ \AA}$ , so that it is well below the detection threshold of the SS92 survey, and most earlier Mg II absorption line surveys. We later realized that this weak system was cataloged by Churchill et al. 1999, at  $z_{abs} = 0.55020$ .

Ignoring for the moment the absence of an identified absorbing galaxy for the  $z_{abs} = 0.6681$  system (there are several candidates without spectroscopic redshifts, albeit at relatively large impact parameters, evident in Figure 4a), the  $z_{abs} = 0.5502$  system is interesting for a number of reasons:

first, the absorption is apparently associated with a much fainter galaxy than the other 4 systems considered in this pilot study, with a circular velocity of only  $v_c \simeq 100 \text{ km s}^{-1}$ . The galaxy is highly inclined ( $\theta_i \simeq 75^\circ$ ), with the projection of the major axis missing the QSO position by only 1.5 arc seconds on the plane of the sky. Despite the high inclination and the projected impact parameter of  $26.5h^{-1} \text{ kpc}$ , the absorption velocity is consistent with the systemic velocity of the galaxy (see Figure 4b), and has a total velocity spread of only  $\sim 50 \text{ km s}^{-1}$ . The implications of the relative kinematics of the absorption and emission will be discussed in §4.4.

There is no information on the H I content of either the  $z_{abs} = 0.5502$  or the  $z_{abs} = 0.6681$  system, despite the existence of HST/FOS spectra, as the continuum of the QSO is cut off shortward of  $\sim 2200 \text{ \AA}$  by a higher redshift Lyman limit system.

### 3.5. Q1317+276 (Ton 153)

SS92 discovered two intermediate redshift absorption systems along this line of sight, at  $z_{abs} = 0.2887$  and at  $z_{abs} = 0.6598$ . An object within about 1 arc second of the QSO sightline is evident in the *HST* image presented in Figure 5a, but no successful spectroscopy has been performed on this object, since the QSO is extremely bright. Earlier spectroscopy from Lick Observatory indicated that both G1 and G2 were consistent with having the same redshift as the  $z_{abs} = 0.6598$  absorption, within the errors (the spectra were of low quality). Because of this ambiguity, the LRIS slit was oriented so as to include both galaxies, and hence is not aligned with the major axis of either galaxy. The new spectra clearly show that G1 (which is both spectroscopically and morphologically of early type) has  $z_{gal} = 0.672$ , which is much too high to be related to the observed absorption. Galaxy G2, on the other hand, has a systemic redshift of  $z_{gal} = 0.6610$ , within  $200 \text{ km s}^{-1}$  of the observed Mg II absorption (see Figure 5b).

Galaxy G2 has a very large projected impact parameter ( $71.6h^{-1} \text{ kpc}$ ) and because of this the identification of it as the galaxy responsible for the absorption is somewhat tentative; however, as for other more secure identifications presented in this paper, the extrema of the absorbing gas velocities are consistent with an extrapolation of the disk kinematics to the large galactocentric distances. In this case, though, attributing the gas to the disk of G2 would imply a de-projected circular velocity of  $\simeq 250 \text{ km s}^{-1}$  (which is quite reasonable for a galaxy of  $\sim 1.6L^*$ ) but implies an extension of the disk-like rotation to a de-projected galactocentric radius of  $\sim 130h^{-1} \text{ kpc}$ , possibly stretching the bounds of feasibility<sup>5</sup>.

The absorbing gas yields a clear detection of Mg I associated with the dominant component of Mg II at  $v_{sys} = -170 \text{ km s}^{-1}$ , and a hint of Mg I in the weaker  $v_{sys} = -80 \text{ km s}^{-1}$  component.

---

<sup>5</sup>The circular velocity implied for G2 is also consistent with the measured rotation curve, although the fact that the slit was placed at an angle of  $\sim 60$  degrees relative to the major axis makes the de-projection of the rotation curve somewhat model-dependent.

There does appear to be significant Mg II absorption all the way to  $v_{sys} = 0$ . This is circumstantial evidence that the gas is indeed dynamically related to galaxy G2. We will discuss this system in more detail in §4.5.

There is a strong Lyman  $\alpha$  absorption line ( $W_{\lambda}^0 = 1.5 \text{ \AA}$ ) associated with the Mg II absorption, and an optically thick Lyman limit (measured by Bahcall et al. 1993 at  $\tau = 3.5$  and Churchill et al. 2000 at  $\tau = 5.4$ ). Given uncertainties in the flux zero point of FOS data, we take these measurements as lower limits, suggesting an H I column density of  $\gtrsim 10^{18} \text{ cm}^{-2}$ ). Interestingly, there is a strong complex of Lyman  $\alpha$  forest lines extending from  $z = 0.660$  to  $z = 0.672$  ( $\sim 2200 \text{ km s}^{-1}$ ; Bahcall et al. 1996) and there are at least 2 galaxies (including the early type G1 1317+276) near the line of sight at  $z \simeq 0.67$ .

#### 4. KINEMATICS

Although the present sample of galaxies is small, there are interesting trends that already suggest that standard interpretation of Mg II kinematics may be inadequate to describe the data. It has become standard to interpret the velocity asymmetries that are typical of Mg II absorption systems (and DLAs) as being consistent with the interception of a rotating disk that is highly inclined with respect to the line of sight (LOS) (e.g., Lanzetta & Bowen 1992; Charlton & Churchill 1998; Prochaska & Wolfe 1997). In the sense that most of the 5 absorbing galaxies observed were selected because they are clearly disk galaxies, it is perhaps not surprising that the kinematics are indeed similar to that expected for disk rotation. Charlton & Churchill (1998) have interpreted many Mg II systems (drawn primarily from the same sample as the present observations) as having a dominant component ascribed to rotation, with additional absorption due to radial infall (i.e., a “halo” component) to explain the weaker “satellite” absorbing components. Components of Mg II absorption ascribed to radial infall or outflow would be expected, on average, to be roughly symmetric with respect to the galaxy systemic redshift. The same would be true if there were a significant component of “halo” gas clouds in random orbits about the galaxy center of mass (see, e.g., Charlton & Churchill 1998).

However, the new information on the systemic velocity and rotation curves for the parent galaxies presents a puzzle: for 4 of the 5 systems (i.e., all but Q1222+228), *all* of the absorbing material lies at velocities offset to one side of the galaxy systemic redshift  $z_{gal}$ . Asymmetric behavior of the absorption line kinematics with respect to galaxy systemic velocities would be a clear prediction of gas clouds embedded in a rotating disk with relatively large inclination angle with respect to the line of sight (cf. Lanzetta & Bowen 1992). However, at the large observed impact parameters to the absorbing galaxies, it is not possible to explain the *range* of velocities  $\Delta v$  spanned by the absorbing material with a thin or even a moderately thick disk model. At large impact parameter, for a highly inclined rotating disk, the sampling of the galaxy rotation curve would be such that only a very small  $\Delta v$ , centered at  $v \simeq v_{rot}$ , would be expected. There are velocity components that would be consistent with an extension of disk kinematics to the line of sight in each case, but

reproducing the *width* of the velocity profiles, given our knowledge of the galaxy geometry, requires an additional component to the kinematic model.

To summarize, the gas-phase kinematics traced by Mg II absorption relative to the galaxy systemic redshift and rotation curves seems to indicate that rotation dominates, but simple disk rotation is inadequate to explain the range of velocities. The fact that even the sub-dominant components of absorption exhibit systematics that are also indicative of a preferred axis of rotation, as opposed to a symmetric distribution of velocities relative to systemic, suggests that absorbing gas has net rotation independent of its location within the galaxy’s gaseous envelope. We now consider a simple kinematic model that allows for rotation-like systematics with the possibility of extending the velocity range of absorbing gas without introducing velocity components on the opposite side of the systemic galaxy redshift  $z_{\text{gal}}$ . These models are similar to those presented by Morton & Blades (1986) to explain the kinematics of Ca II absorption toward stars in the Galactic halo.

We assume a co-rotating thick disk (as has often been invoked in studies of high ionization species in the Galactic halo—see, e.g., Savage, Sembach, & Lu 1997), where the effective thickness  $H_{\text{eff}}$  in the  $z$  direction is a free parameter, and a flat rotation curve throughout. The non-negligible thickness allows for a larger range of velocities to be sampled by a line of sight intersecting it, as long as the inclination angle  $\theta_i$  with respect to the plane of the sky is non-zero. The assumed rotation curve is given by:

$$\vec{V}_\phi(r) = v_c \hat{\phi} \quad (1)$$

where  $r$  is a radial coordinate measured in the plane of the galaxy disk and  $\hat{\phi}$  is the tangential direction.

In Cartesian coordinates:

$$\vec{v} = \frac{-y}{r} v_c \hat{x} + \frac{x}{r} v_c \hat{y} \quad (2)$$

The coordinates are defined so that the value of  $x$  is constant along the line of sight,  $x = p$ , where  $p$  is the impact parameter measured along the major axis of the galaxy (see Figure 6). The line of sight is parallel to the  $y$ - $z$  plane, as illustrated in Figure 6.

We describe the line of sight by a vector of the form:

$$\vec{\mathbf{L}} = -\sin\theta_i \hat{y} - \cos\theta_i \hat{z} \quad (3)$$

where  $z$  is the coordinate measured perpendicular to the disk plane of the galaxy. Projecting the velocity vector above along the LOS vector yields:

$$v_{\text{los}} = \frac{-v_c \sin\theta_i}{\sqrt{1 + (\frac{y}{p})^2}} \quad (4)$$

We make the model more general by introducing a  $z$ -dependence of the rotational speed at a given radial distance from the disk rotation axis. The model is parameterized by a simple exponentially declining velocity with an adjustable velocity scale height.

$$v_\phi(r, z) = v_c e^{-(|z|/h_v)} \hat{\phi} \quad (5)$$

where  $h_v$  is the velocity scale height,  $v_c$  is the measured circular velocity at mid-plane, and  $z$  is the height above the mid-plane of the disk. The line of sight velocity as a function of  $y$  is then given by:

$$v_{\text{los}} = \frac{-v_c \sin\theta_i}{\sqrt{1 + \left(\frac{y}{p}\right)^2}} e^{-(|y-y_0|/(\tan\theta_i h_v))} \quad (6)$$

where the minus sign indicates the sense of rotation. The parameter  $y_0$  is the  $y$  value of the intersection of the line of sight with the mid-plane of the disk (see the diagram in Figure 6). The range of  $y$  values encountered as the line of sight pierces the gas distribution surrounding the galaxy then ranges from  $y_0 - H_{\text{eff}} \tan\theta_i$  to  $y_0 + H_{\text{eff}} \tan\theta_i$ . In terms of the  $y$  coordinate, the distance along the line of sight, relative to the point where it intersects the projection of the disk mid-plane, is then just  $D_{\text{los}} = (y - y_0)/\sin\theta_i$ .

With direct measurements of  $\theta_i$ ,  $p$ ,  $y_0 \cos\theta_i$  from the HST images, and the circular velocity  $v_c$  from the optical rotation curves (all measured values are summarized in Table 5), the only free parameters in these simple models are the assumed disk thickness  $H_{\text{eff}}$  which controls the range of  $y$  values considered, and the velocity scale height  $h_v$ .

Our approach in fitting the models was to adjust the two parameters  $H_{\text{eff}}$  and  $h_v$  to try to match the observed gas-phase kinematics. We have made no assumptions about the distribution of Mg II absorbing clouds as a function of  $z$  distance or  $r$  with respect to the center of each galaxy. Instead, for simplicity, we treat  $H_{\text{eff}}$  as the effective thickness of the gas layer capable of giving rise to detectable Mg II absorption and so we neglect the path length differences through various parts of the gas layer. In some cases there are many combinations of  $h_v$  and  $H_{\text{eff}}$  that are in reasonable agreement with the observed velocities of the absorbing gas, while in other cases the allowed range of parameters is very small. We discuss each case individually below, and illustrate particular models that come closest to agreement with the data in Figure 7. The adopted parameters that were used to produce the plots shown in figure 7 are summarized in table 6.

#### 4.1. Q0827+243

The large velocity range ( $\simeq 270 \text{ km s}^{-1}$ ) observed in the absorption profile of G1 0827+243 cannot be reproduced by any thick disk model without incorporating a declining rotation speed as a function of  $z$  distance. The model shown in figure 7a, which accounts for most of the observed

velocity of the absorbing gas, is not unique— a similar velocity range can be produced by any model for which  $h_v$  is small compared to  $H_{\text{eff}}$  (i.e., where there is gas with essentially all velocities between  $-250 \text{ km s}^{-1}$  and  $20 \text{ km s}^{-1}$  with respect to systemic along the line of sight) and the effective thickness of the gas layer  $H_{\text{eff}} \geq 5h^{-1} \text{ kpc}$ .

The fact that the maximum velocity in absorption exceeds the projected rotation curve may mean either that the rotation speed of the galaxy has been under-estimated, or that there is a turbulent component of velocity which adds  $\sim 50 \text{ km s}^{-1}$  to the gas-phase near the intersection with the disk. As discussed above, the galaxy is apparently being disturbed by a smaller satellite galaxy, and the galaxy is by far the most actively star forming, judging by the equivalent width of the [OII]  $\lambda 3727$  emission line, in the present sample. Both of these phenomena may contribute to the gas-phase kinematics.

#### 4.2. Q1038+064

The velocity profile of G1 1038+064 is well-reproduced by models in which  $h_v$  is of the same order as  $H_{\text{eff}}$  and  $H_{\text{eff}} \geq 2h^{-1} \text{ kpc}$ . Gas with the largest departure in line-of-sight velocity relative to systemic is predicted by this family of models to lie in the plane of the galaxy, so that it is quite reasonable to use the absorption line velocities to extend the galaxy rotation curve to  $45h^{-1} \text{ kpc}$  as discussed in §3.2. Nevertheless, it is somewhat surprising to observe disk kinematics in gas with such small H I column density (see §3.2).

#### 4.3. Q1148+387

It is difficult to reproduce the full velocity range of  $\Delta v \simeq 160 \text{ km s}^{-1}$  with our kinematic model. The most successful model is one in which the effective gas layer is very thick ( $\gtrsim 25h^{-1} \text{ kpc}$ ) and has a constant rotational velocity with  $z$  distance (as in figure 7c). With this model, the extreme value of the line of sight velocity reaches only  $-120 \text{ km s}^{-1}$  with respect to systemic (although the extension to zero systemic velocity is reproduced) and most of the absorption occurs substantially away from the plane of the disk, which may be unphysical. Models with relatively thin gas layers and small velocity scale heights, which work for the two previous cases, are very unsuccessful for G1 1148+387. It is possible that models in which the angular momentum vector for “halo” gas has a different direction than that of the disk would be more successful. We merely point out that application of our simple kinematic model leads to a relatively poor agreement with the observations and a somewhat implausible physical situation.

#### 4.4. Q1222+228

The difficulty for this system is that the galaxy is nearly edge-on and yet the absorption kinematics are centered at the systemic velocity of the galaxy. Thus, it is necessary to keep the extension of the disk which carries the full rotation speed of the galaxy very thin to prevent absorption components with high negative velocities. At the same time, the total thickness of the gas layer, if associated with a thick disk, must be large enough to allow for absorbing gas  $\sim 5$  kpc above the projection of the disk plane. Reasonably successful models are those with  $H_{\text{eff}} \leq 5h^{-1}$  kpc and velocity scale heights that are very small,  $h_v \leq 0.1h^{-1}$  kpc. Such a kinematic model produces gas that asymptotes quickly to zero systemic velocity only a few kpc above the disk plane.

It is notable that the Mg II absorption for this system is much weaker, and the galaxy considerably fainter, than for the others considered here.

#### 4.5. Q1317+276

Reproducing the large departure of the measured absorbing galaxy velocities from systemic requires gas at large  $z$  distances above the plane to have very close to the full circular velocity of the galaxy. Because the line of sight through the galaxy is nearly parallel to the galaxy minor axis, material in the plane of the disk cannot contribute to the observed velocities. For the model shown in figure 7e, most of the absorption at non-zero systemic redshifts arises in material very nearly directly above the center of the galaxy rotation axis (i.e., very small values of  $y$ —see figure 6) which is rather unphysical (recall that we have assumed a constant rotational velocity, which is acceptable at large galactocentric distances).

As discussed in §3.5, the identification of galaxy G2 1317+276 as the one responsible for the absorption must be considered tentative. Nevertheless, there is gas at velocities that range from systemic to a maximum velocity that is very similar to the maximum rotation speed that could be seen associated with G2 1317+276 given the inclination angle. This system would seem to be one in which domination by “halo” velocity components might be the most reasonable, but once again the absence of gas at positive velocities with respect to systemic is puzzling.

### 5. DISCUSSION

We have presented data on 5 intermediate redshift Mg II absorption systems for which there is much more information than has been available in the past, and in many ways it has made for a more puzzling picture of the nature of absorbing material in the outer parts of (in these cases, disk) galaxies. Most recent models for the kinematics of Mg II absorption systems have involved two separate components contributing to the kinematics— a rotating disk component, which is thought



to produce the “dominant” components of complex kinematic systems (e.g. Charlton and Churchill 1998, Churchill & Vogt 2001), with more symmetrical (with respect to the systemic redshift) “halo” components providing a broad distribution of velocity, whose origins might be ascribed to random motions, infall, or outflow. Given the limited geometrical information from Mg II–selected galaxy surveys (Steidel et al. 1997, SDP, Bergeron & Boissé 1991) at these redshifts, and the limited morphological information on the absorbing galaxies (Steidel 1998; Steidel et al. 1997), this picture has the advantage of being compatible with both the spiral nature of most of the galaxies, and the large (and possibly quasi-spherical) gaseous envelopes surrounding a very large fraction of  $z \sim 0.6$  field galaxies within  $\sim 1.5$  magnitudes of present-day  $L^*$ .

However, based on the systems presented in this paper, the situation cannot be so simple—the components that are not easily explained by thin disk rotation must have the systematics that are like those produced by rotation. There is clear evidence for rotation in 4 out of the 5 cases, since not only is all of the absorption offset to one side of the systemic redshift, in all cases it is in the right sense to be qualitatively explained by an extension of the disk rotation to the line of sight (which is well beyond where the optical rotation curves are measured, by factor of 2 to as much as a factor of 6). As detailed in §4, though, given knowledge of the disk inclinations and impact parameters (not known for previous analyses of Mg II kinematics), disk–like rotation is not enough to explain the bulk of kinematic components seen in absorption. Our simple kinematic modeling of rotating “thick disks” in §4 (which are by no means intended to be unique solutions to the kinematic conundrum) imply that for two of the galaxies (G1 1148+3842 and G2 1317+276) a successful model does not involve an extension of the disk at all, but requires essentially a *rotating halo*. In the three other cases, the observed kinematics are reasonably well fit by thick disk models in which the circular velocities are a rapidly decreasing function of scale height, with the extrema of the velocities being produced at the disk intersection, but where the gas at lower relative velocities with respect to systemic comes from fairly large  $z$  distances. As discussed in §4, the galaxies best–fit with the velocity scale height models allow for a wide range of solutions so long as the ratio  $H_{\text{eff}}/h_v$  remains roughly constant, as there are only weak constraints on the required thickness of the gas layer above the extrapolation of the plane of the disk. Given what is known about the geometry of the gaseous envelopes capable of giving rise to easily detectable Mg II absorption, we would be inclined to favor models in which  $H_{\text{eff}}$  is on the order of  $\sim 30 - 40h^{-1}$  kpc for  $L^*$  galaxies like G1 1038+064 and G1 0827+243. On the other hand, G2 1222+228, which is among the faintest Mg II absorbers identified at comparable redshift, must be quite different from these larger spirals, in that the effective thickness of the disk must be quite thin to *avoid* producing absorption at large velocities with respect to systemic, and the velocity scale height must be even smaller to bring the kinematic model into tolerable agreement with the data.

It is instructive to consider possible local analogs of the kinematic behavior of galactic gas we observe at  $z \sim 0.5$ . For highly ionized gas in the Galaxy seen in absorption against the continua of hot stars and extragalactic AGN, a model in which the “halo” gas co-rotates with the disk up to heights of several kpc above the plane has often been assumed, and recent observations seem to

require this (Savage, Sembach, & Lu 1997). The scale heights reached appear to vary as a function of the ionization state of the ion, with the most highly-ionized species extending to the largest distances above the plane. However, in at least 2 of the cases we have observed, Mg II would have to have an effective scale height that is more than an order of magnitude larger than that of C IV in the Galaxy, and in the other cases a completely co-rotating halo would fail badly to reproduce the observed absorption line kinematics.

A recent development based on the most sensitive H I (e.g., Swaters, Sancisi, & van der Hulst 1997; Sancisi et al. 2000, Schaap, Sancisi, & Swaters 2000) and H II (e.g., Rand 2000) measurements locally is the ability to follow the kinematics of the gas to relatively large  $z$  distances above the planes of spiral galaxies. Rand (2000) finds that for the edge-on starburst galaxy NGC 5775, there is gas whose rotation velocity has decreased to zero by a height of 5 kpc. He interprets this behavior as a trend of decreasing rotational velocity as a function of  $z$ , similar to our modeling above. Swaters et al. (1997) observed clear evidence for a systematically smaller rotation velocity of the “H I halo” of NGC 891, with gas at several kpc above the plane rotating 25–50 km s<sup>-1</sup> more slowly than in the plane. Sancisi et al. (2000) discuss 21-cm observations of galaxies with “beards”, in which gas observed away from the plane of the galaxy seems to “know” about the rotation of the disk (i.e., the rotation has the same general direction as far as can be discerned with the observations) but has kinematics that represent large departures from the disk rotation. The qualitative similarities of these observations to those presented in this paper are clear; however, it is unclear how common the kinematically “anomalous” gas is in local spirals (only a few galaxies have been observed to the required level of sensitivity). In any case, the gas-phase kinematics of  $z \sim 0.5$  galaxies refer to much larger galactocentric distances and much smaller H I column densities (with the exception of G1 0827+243 which would easily be observed in 21 cm emission if it were nearby).

The interpretation of the slowly rotating gas in nearby galaxies is largely qualitative at the present time— the authors cited above invoke both hydrodynamic disk/halo cycling of gas, and changes in the gravitational potential with  $z$  distance above the plane, as possible explanations of the observations. If the higher redshift objects are at all analogous, it is hard to imagine that the gravitational potential argument can be relevant, since the sight lines all intersect the galaxies at radii where dark matter would be expected to dominate strongly over a baryonic disk.

Bregman (1980) considered kinematic models of the disk/halo circulation (the “Galactic fountain” model) in which parcels of hot gas are expelled from the disk by star formation events and may, by the time they cool, have been transported to both a large height above the plane and to a larger distance from the galaxy rotation axis. Because of conservation of angular momentum, the gas at large heights above the galactic plane would lag with respect to the disk rotation, producing a more slowly-rotating “halo”. In practice, the kinematics of the gas as a function of height  $z$  would depend on the details of the distribution and energetics of previous star-formation episodes and on the pressure profile of the galaxy as a function of galactocentric distance; in principle, gas with any velocity between systemic and  $v_c \sin \theta_i$  could be observed at any position along the line of sight. Nevertheless, as long as the rotation of the gas dominates over radial motions (infall or

outflow) such a picture would be qualitatively consistent with our observations. In the nearby starburst galaxies discussed above, very active current star formation lends qualitative credence to fountain flows as a possible explanation of the observed gas-phase kinematics, but this leads to a puzzle for the higher redshift objects– with the exception of G1 0827+243, none of the galaxies considered here has an unusually high rate of star formation, and certainly there is no active star formation coinciding with the large inferred disk impact parameters. The observation that the Mg II absorbers at intermediate redshift tend in general *not* to be particularly active star-formers has been used previously to argue against fountain-type flows being important to the presence of extended gaseous envelopes (SDP, Steidel 1995), but this argument assumes that the timescale for the circulation of the gas is relatively short. We now consider the possibility that past star formation, now observed only through the older stellar populations present in the galaxies, might be responsible for the rotating halo gas observed at  $z \sim 0.5$ .

There is mounting evidence for the importance of large-scale galactic winds for star forming galaxies at high redshift. Observations of  $z \gtrsim 3$  Lyman break galaxies show clearly that the strong far-UV interstellar absorption lines are blue-shifted, and the Lyman  $\alpha$  emission lines red-shifted, by up to  $1000 \text{ km s}^{-1}$  with respect to systemic (Pettini et al. 1998, 2001), with typical implied outflow velocities being several hundred  $\text{km s}^{-1}$ . Very recently, it has been shown that the properties of the Lyman  $\alpha$  forest are strongly affected by the presence of LBGs  $z \sim 3$ , and that several different observations can be explained simultaneously if the super-winds have a sphere of influence of  $\sim 125h^{-1} \text{ kpc}$  on average (Adelberger et al. 2001). The cooling time for the shock heated gas in the halo can be very long, and it is at least conceivable that this gas, or similar gas ejected at lower redshifts (where there are currently fewer observations constraining the extent of super-winds), could ultimately supply the gas that forms the bulk of the disk observed at  $z \sim 0.5$  and the material that produces Mg II absorption. The physics of the multi-phase gas that no doubt results from the wind activity is very complex, and a full treatment is well beyond the scope of this paper. It is not clear that this kind of flow would really result in a “memory” of disk-like kinematics in the halo, since the material involved in the type of super-winds inferred to exist at  $z \sim 3$  would tend to originate from low angular momentum gas that has settled to a very compact nuclear region where most of the star formation appears to take place. An alternative possibility is that the gas has acquired significant angular momentum during the extended time that it spends at large galactocentric distances, and that this angular momentum is naturally strongly correlated with that of the gas that has found its way to the disk. In this scenario, much of the gas falling onto the disk would do so gradually, would be significantly metal-enriched, and would have the same kinematic systematics as disk gas, albeit with smaller rotational velocities. It is not entirely clear whether the observed kinematics at  $z \sim 0.5$  are consistent with both rotation *and* infall; the sample is too small to justify a more in-depth treatment at this time. In any case, a general picture of halo gas being “recycled” disk gas may actually help explain the loose correlation of inferred size of the Mg II-absorbing envelope with stellar mass, the inferred roughly axisymmetric geometry of the envelope, and the persistence of absorbing gas over much longer than the typical galaxy dynamical time of  $\sim$  a few  $\times 10^8$  years.

It is almost certainly premature to generalize about the nature of the Mg II absorbing gas, given the small sample of 5 systems presented here and the fact that each system requires somewhat different assumptions to find kinematic models that are adequate. We have not considered in detail whether any of these ad hoc kinematic models are physically plausible, and we have not considered the hydrodynamics of the gas at all. More detailed modeling seems unjustified until a larger sample is in hand. It is clearly worth extending this type of study in two ways. First, it is essential to obtain accurate redshifts and (where possible) rotation curves for a larger sample of Mg II–selected galaxies (the HIRES and WFPC-2 data are already on hand for a sample of  $\sim 25$  Mg II absorbers). Secondly, it will be important to obtain high quality absorption line data extending to higher ionization species (like C IV) to see if the rotation signatures are as clear in the highly ionized component as they are for the gas presently traced by Mg II. Initial forays in this direction have already been made by Churchill et al. (2000), but the archival FOS data are generally of too-coarse resolution to compare absorption line kinematics in detail. On the other hand, a fraction of the QSOs in the sample for which we have WFPC-2 images are bright enough for STIS high dispersion spectroscopy in reasonable integration times, and this should prove a fruitful line of research in the future.

We would like to thank Kurt Adelberger for help with the observations and for many discussions. Useful conversations with Betsy Barton-Gillespie, Liese van Zee, and Jason Prochaska are gratefully acknowledged. CCS and AES have been supported in part by grants AST95-96229 and AST-0070773 from the U.S. National Science Foundation and by the David and Lucile Packard Foundation. Early work on the HST data was supported by grant GO-05984.01-94A and GO-06577.01-95A from the Space Telescope Science Institute.

## REFERENCES

- Adelberger, K.L., Steidel, C.C., Shapley, A.E., & Pettini, M. 2001, *ApJ*, submitted
- Bahcall, J.N., et al. 1993, *ApJS*, 87, 1
- Bahcall, J.N., et al. 1996, *ApJ*, 457, 19
- Bergeron, J. & Boissé, P. 1991, *A&A*, 243, 344
- Blanton, M., et al. 2001, *AJ*, 121, 2358
- Bowen, D.V., Tripp, T.M., & Jenkins, E.B. 2001, *AJ*, 121, 1456
- Bregman, J.N. 1980, *ApJ*, 236, 577
- Burbidge, E.M., Smith, H.E., Weymann, R.J., & Williams, R.E. 1977, *ApJ*, 218, 1
- Charlton, J. C., & Churchill, C. W. 1996, *ApJ*, 465, 631
- Charlton, J. C., & Churchill, C. W. 1998, *ApJ*, 499, 181

- Churchill, C.W., & Vogt, S.S. 2001, *AJ*, 122, 679
- Churchill, C.W., Rigby, J.R., Charlton, J.C., & Vogt, S.S. 1999, *ApJS*, 120, 51
- Churchill, C. W., Mellon, R. R., Charlton, J. C., Jannuzi, B. T., Kirhakos, S., Steidel, C. C., & Schneider, D. P. 2000, *ApJ*, 543, 577
- Churchill, C. W., Steidel, C. C., & Vogt, S. S. 1996, *ApJ*, 471, 164
- Dickinson, M., & Steidel, C.C. 1996, in *New Light on Galaxy Evolution*, eds. R. Bender & R. Davies (Kluwer: Dordrecht), 295
- Folkes, S. et al. 1999, *MNRAS*, 308, 459
- Fruchter, A.S., & Hook, R.N. 1997, *SPIE*, 3164, 120
- Haehnelt, M., Steinmetz, M., & Rauch, M. 1998, *ApJ*, 495, 647
- Lanzetta, K. M., & Bowen, D. V. 1992, *ApJ*, 391, 48
- Le Brun, V., Bergeron, J., Boissé, P., & Deharveng, J. M. 1997, *A&A*, 321, 733
- Lilly, S.J., Le Fèvre, O., Hammer, F., & Crampton, D. 1996, *ApJ*, 460, L1
- McDonald, P., & Miralda-Escudé, J. 1999, *ApJ*, 519, 486
- Morton, D.C., & Blades, J.C. 1986, *MNRAS*, 220, 927
- Oke, J.B., et al. 1995, *PASP*, 107, 3750
- Petitjean, P., & Bergeron, J. 1990, *A&A*, 231, 309
- Pettini, M., Shapley, A.E., Steidel, C.C., Cuby, J.G., Dickinson, M., Moorwood, A.F., Adelberger, K.L., & Giavalisco, K.L. 2001, *ApJ*, 554, 981
- Pettini, M., Kellogg, M., Steidel, C.C., Dickinson, M., Adelberger, K.L., & Giavalisco, M. 1998, *ApJ*, 508, 539
- Prochaska, J.X., & Wolfe, A.M. 1998, *ApJ*, 507, 113
- Prochaska, J.X., & Wolfe, A.M. 1997, *ApJ*, 487, 73
- Rand, R. 2000, *ApJ*, 537, 13
- Rao, S. M., & Turnshek, D. A. 2000, *ApJS*, 130, 1
- Sancisi, R., Fraternali, F., Oosterloo, T., & van Moorsel, G. 2000, in *Gas and Galaxy Evolution*, eds. J. Hibbard, M. Rupen, and J. van Gorkom, in press (astro-ph/0009119)
- Savage, B.D., Sembach, K.R., & Lu, L. 1997, *AJ*, 113, 2158
- Schaap, W.E., Sancisi, R., & Swaters, R.A. 2000, *A&A*, 356, 49
- Steidel, C. C. 1995, in *QSO Absorption Lines*, ed. G. Meylan (Garching : Springer Verlag), 139
- Steidel, C. C. 1998, in *Galactic Halos: A UC Santa Cruz Workshop*, ASP Conf. Series, V136, ed. D. Zaritsky (San Francisco : PASP), 167

- Steidel, C. C., Dickinson, M., Meyer, D. M., Adelberger, K. L., & Sembach, K. R. 1997, *ApJ*, 480, 568
- Steidel, C.C., Pettini, M., Dickinson, M., & Persson, S. 1994, *AJ*, 108, 2046
- Steidel, C. C., Dickinson, M. & Persson, E. 1994, *ApJ*, 437, L75
- Steidel, C. C., & Sargent, W. L. W. 1992, *ApJS*, 80, 1 (SS92)
- Swaters, R., Sancisi, R., & van der Hulst, J.M. 1997, *ApJ*, 491, 140
- Turnshek, D.A., Rao, S., Nestor, D., Lane, W., Monier, E., Bergeron, J., & Smette, A. 2001, *ApJ*, 553, 288
- Vogt, N.P., Forbes, D.A., Phillips, A.C., Gronwall, C., Faber, S.M., Illingworth, G.D., & Koo, D.C. 1996, *ApJ*, 465, 15
- Vogt, S. S., et al. 1994, in *Proceedings of the SPIE*, 2128, 326
- Weymann, R.J., Williams, R.E., Peterson, B.M., & Turnshek, D.A. 1979, *ApJ*, 233, 43
- Wolfe, A.M., & Prochaska, J.X. 2000, *ApJ*, 545, 603
- Wolfe, A.M., Turnshek, D.A., Smith, H.E., & Cohen, R.D. 1986, *ApJ*, 294, 67
- Young, P., Sargent, W.L.W., & Boksenberg, A. 1982, *ApJS*, 48, 455

Table 1. Absorbing Galaxy Properties

Object	$z_{\text{gal}}$	$\mathcal{R}_{\text{AB}}^{\text{a}}$	$\mathcal{R}_{\text{AB}} - K$	$\theta^{\text{b}}$	d (kpc) <sup>c</sup>	$M_{\text{B}}^{\text{d}}$
G1 0827+243	0.5258	20.83	3.88	5.8	25.4	−19.98
G1 1038+064	0.4432	20.95	4.45	9.7	38.8	−19.58
G1 1148+387	0.5536	21.59	3.49	3.2	14.4	−19.33
G1 1222+228	0.5502	22.82	4.02	5.9	26.5	−18.09
G2 1317+276	0.6610	21.54	3.84	14.7	71.6	−19.95

<sup>a</sup>From ground-based photometry; the  $\mathcal{R}$  filter has an effective wavelength of 6830 Å close to the HST F702W filter used with WFPC-2.

<sup>b</sup>Projected angular separation of absorbing galaxy from QSO sightline, in arc seconds.

<sup>c</sup>Projected proper separation of galaxy from QSO sightline, in  $h^{-1}$  kpc, for  $\Omega_m = 0.3, \Omega_\Lambda = 0.7$  cosmology.

<sup>d</sup>Absolute rest-frame B magnitude of galaxy, for  $h = 1, \Omega_m = 0.3, \Omega_\Lambda = 0.7$ .

Table 2. WFPC-2 Observations

Field	Date (UT)	Exposure (s)	$\theta_i$ (deg) <sup>a</sup>
Q0827+243	1995 May 29	4600	69
Q1038+064	1995 May 31	4600	60
Q1148+387	1995 May 31	4700	40
Q1222+228	1997 June 11	5000	75
Q1317+276	1995 June 01	4800	58

<sup>a</sup>Galaxy inclination angle with respect to the plane of the sky, estimated from elliptical isophote fits to the WFPC-2 image of each galaxy

Table 3. LRIS Absorbing Galaxy Spectroscopy

Object	$z_{\text{gal}}$	Date (UT)	$\lambda$ Range (Å)	Exposure (s)	PA (deg)
G1 0827+243	0.5259	1999 Mar 18	5400–7960	2400	72.3 (mask)
G1 1038+064	0.4428	1999 Mar 19	4980–7530	2400	73.6 (mask)
G1 1148+387	0.5534	1999 Mar 19	5190–7760	2400	89.0 (longslit)
G1 1222+228	0.5502	1999 Mar 19	5450–8020	2400	34.6 (longslit)
G2 1317+276	0.6606	1999 Mar 18	5770–8340	1200	177.7 (longslit)

Table 4. HIRES QSO Spectroscopy

QSO	$z_{em}$	Date (UT)	$\lambda$ Range ( $\text{\AA}$ )	Exposure (s)
Q0827+243	0.909	1998 Feb 27	3215–5606	7200
Q1038+064	1.270	1998 Mar 01	3975–6408	7200
Q1148+387	1.303	1995 Jan 24	3987–6424	5400
Q1222+228	2.040	1995 Jan 23	3810–6305	3600
Q1317+276	1.022	1995 Jan 23	3810–6305	3600

Table 5. Measured Model Inputs

Object	$\theta$ (deg)	$v_c$ ( $\text{km s}^{-1}$ )	$p^a$ ( $\text{h}^{-1}$ kpc)	$y_0^b$ ( $\text{h}^{-1}$ kpc)
G1 0827+243	69	260	25.3	5.6
G1 1038+064	60	260	37.4	7.9
G1 1148+387	40	195	6.5	17.2
G1 1222+228	75	100	25.0	6.0
G2 1317+276	58	250	0.3	135.1

<sup>a</sup>This is the projected galactocentric distance, measured along the major axis of the galaxy, at the point tangent to the line of sight (see §4 and Figure 6).

<sup>b</sup>The  $y$  value of the intersection of the line of sight with the mid-plane of the galaxy (see §4 and Figure 6).

Table 6. Model Galaxy Parameters

Object	$H_{\text{eff}}$ ( $\text{h}^{-1}$ kpc)	$h_v$ ( $\text{h}^{-1}$ kpc)
G1 0827+243	10	5
G1 1038+064	6	5
G1 1148+387	50	*
G1 1222+228	6	0.1
G2 1317+276	100	*

\*Asterisks indicate cases for which the kinematics are better fit using  $h_v \gg H_{\text{eff}}$ , which is mathematically equivalent to thick disk with constant rotational velocity.



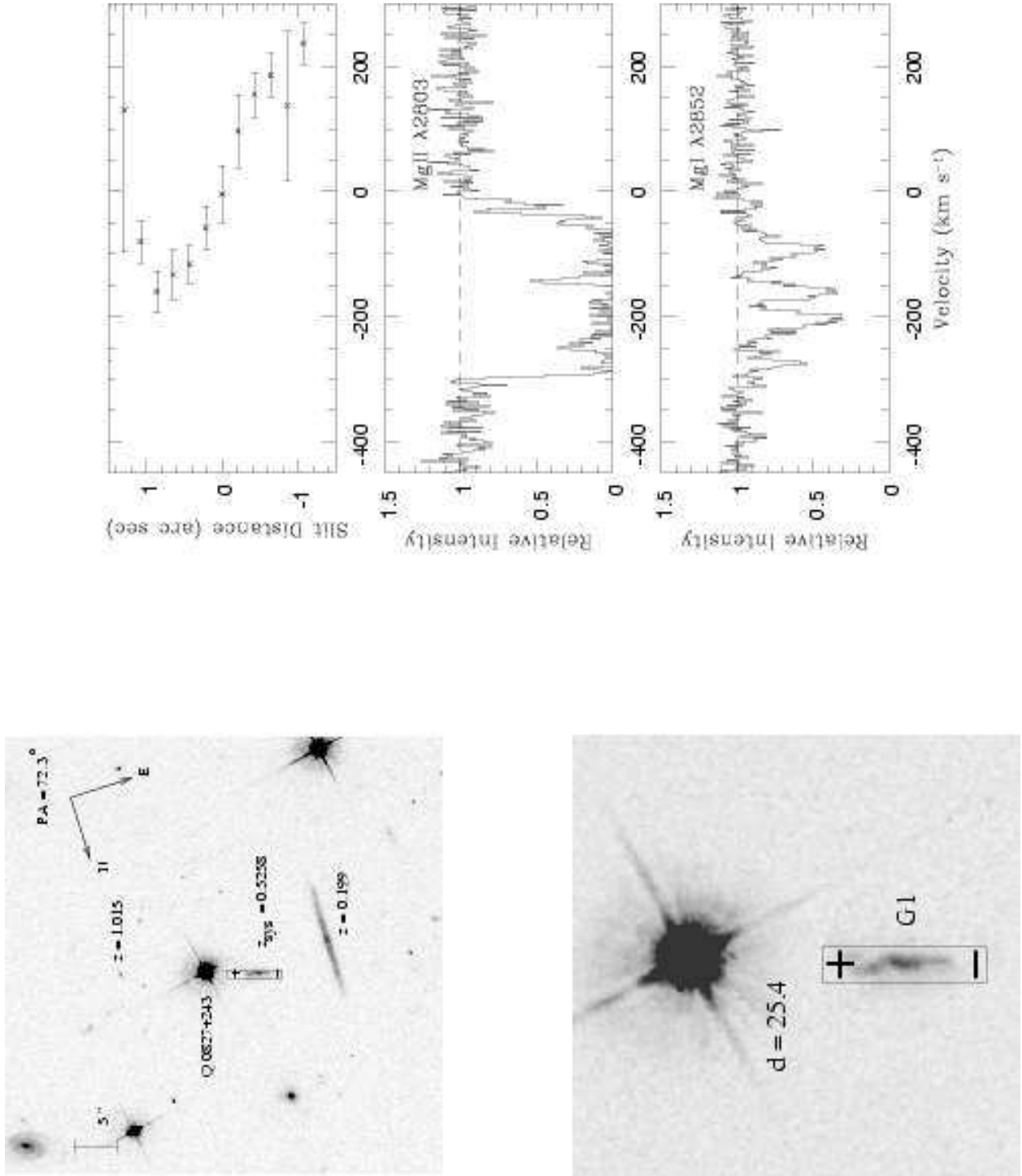


Fig. 1.— a) HST/WFPC-2 F702W images of Q0827+243. The slit position used for the galaxy spectroscopy is indicated; the relative spatial position along the slit is indicated with “+” and “-”, with “+” referring to positive spatial positions, as shown in panel b). b) the observed rotation curve (top) of G1 0827+243, and the kinematics of the observed absorption (middle, bottom) from the HIRES spectrum of the QSO. Note the perturbation of the galaxy kinematics at positive spatial positions, possibly caused by the discrepant velocity of the satellite galaxy that is apparent in Figure 1a. The projected distance ( $d$ ) in  $h^{-1}$  kpc between the QSO sightline and the absorbing galaxy is also indicated.

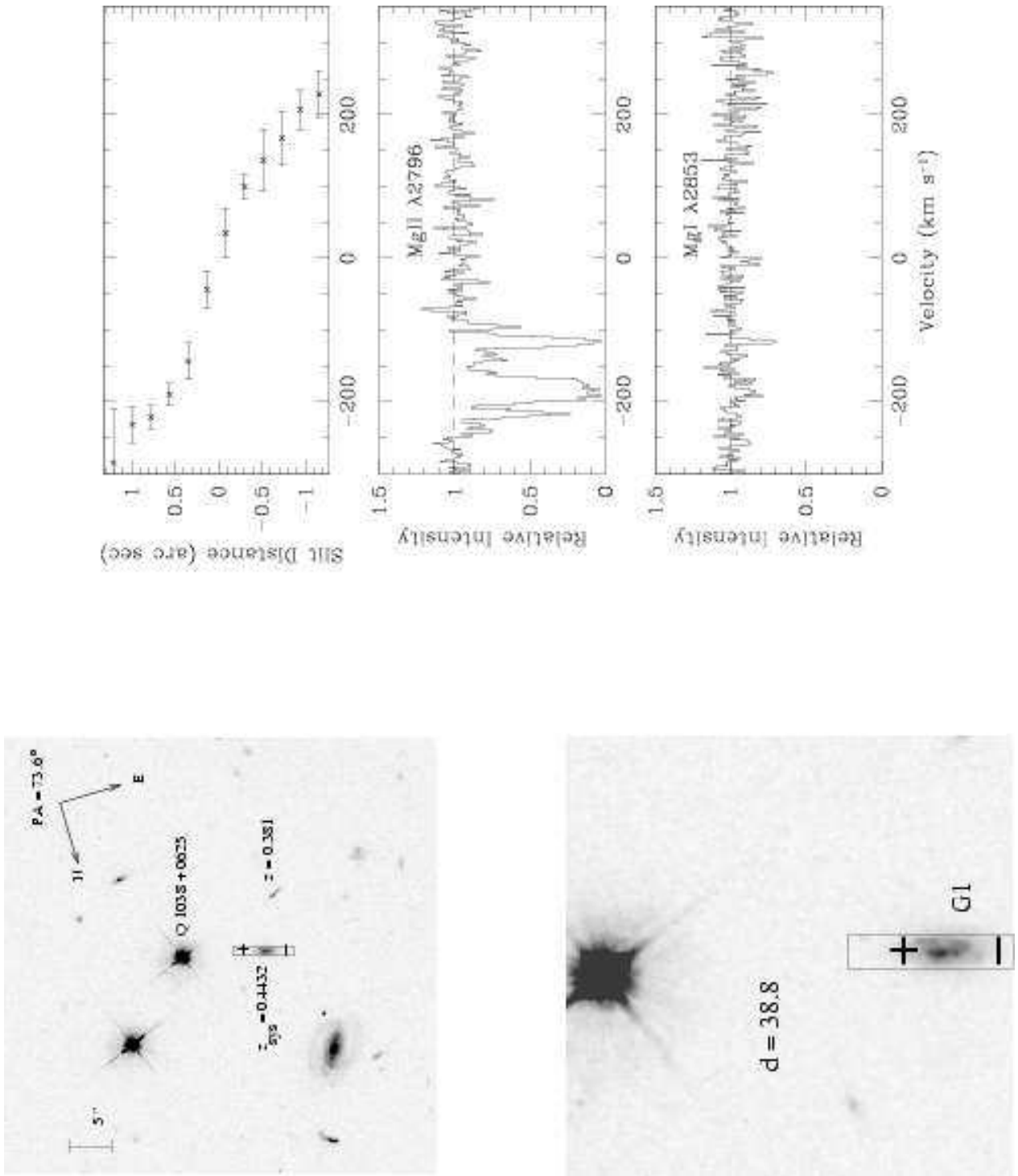


Fig. 2.— a) Same as figure 1, for Q1038+064 b) the observed rotation curve (top) of G1 1038+064, and the kinematics of the absorption (middle, bottom) from the HIRES spectrum of the QSO.

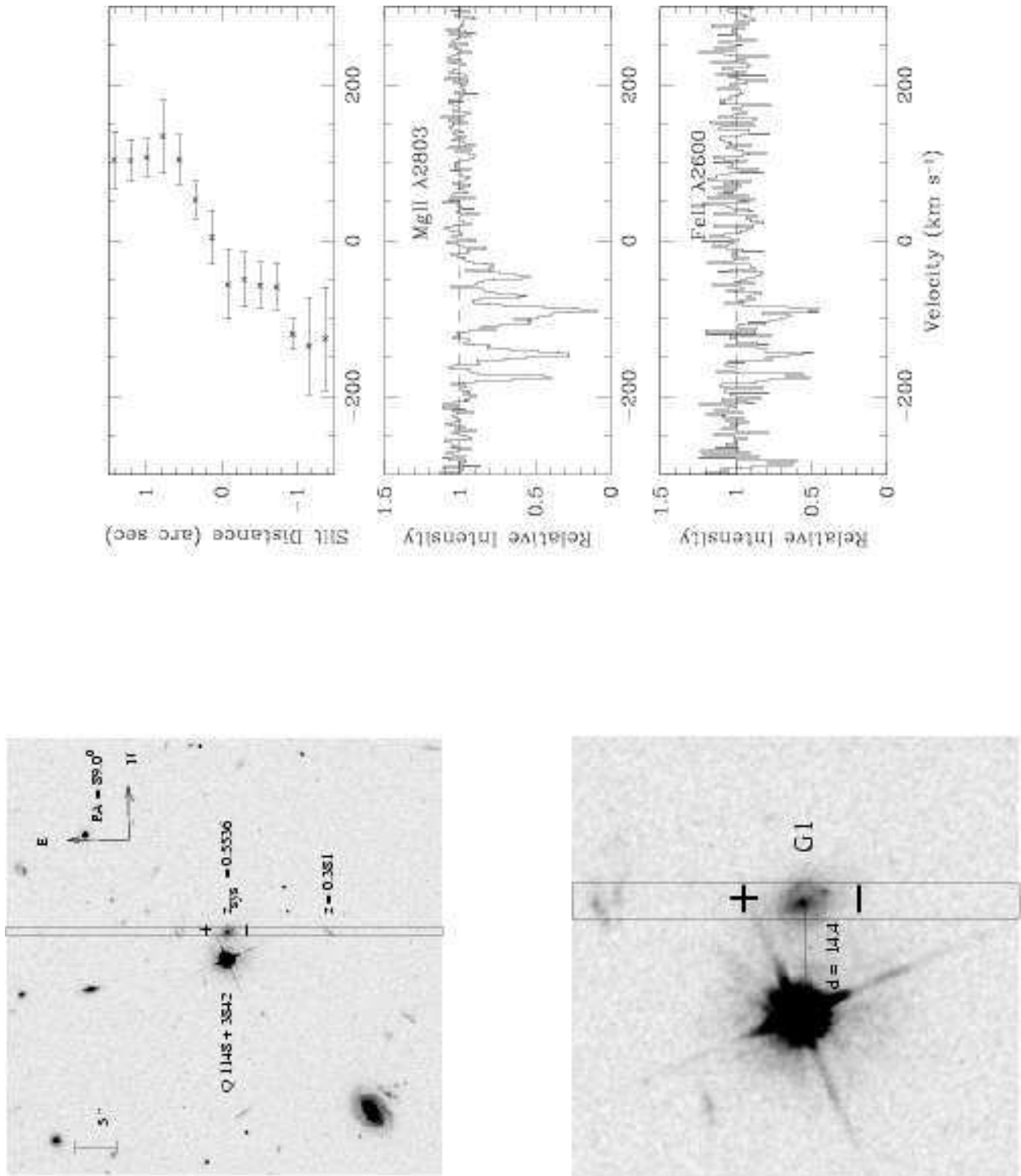


Fig. 3.— a) Same as figure 1, for Q1148+387 b) the observed rotation curve (top) of the G1 1148+3842, and the kinematics of the absorption (middle, bottom) from the HIRES spectrum of the QSO.

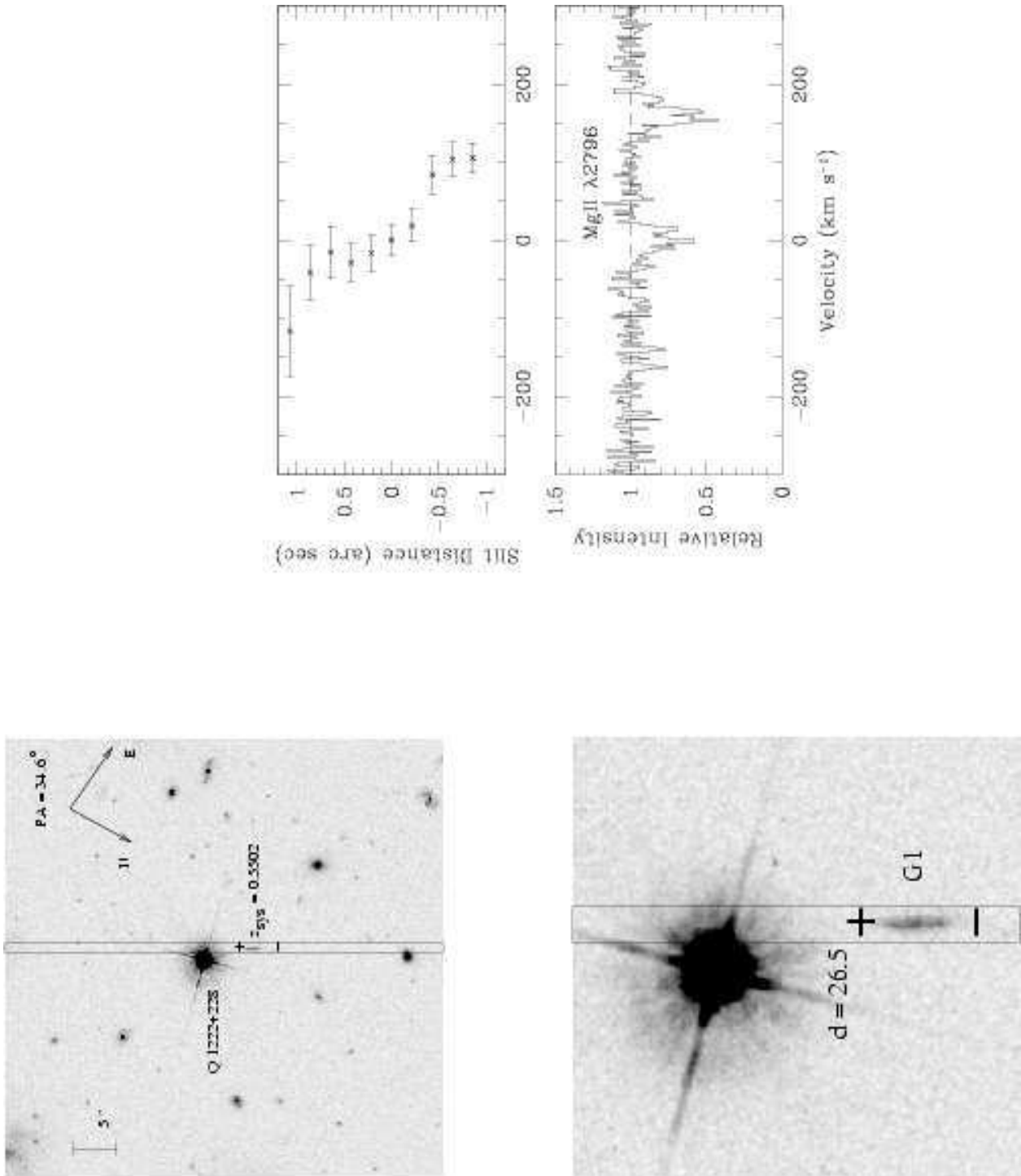


Fig. 4.— a) Same as figure 1, for Q1222+228. b) the observed rotation curve (top) of the G1 1222+228, and the kinematics of the absorption (middle) from the HIRES spectrum of the QSO. The feature that appears in the middle panel near +150 km s<sup>-1</sup> is from a different redshift system and so should be ignored.

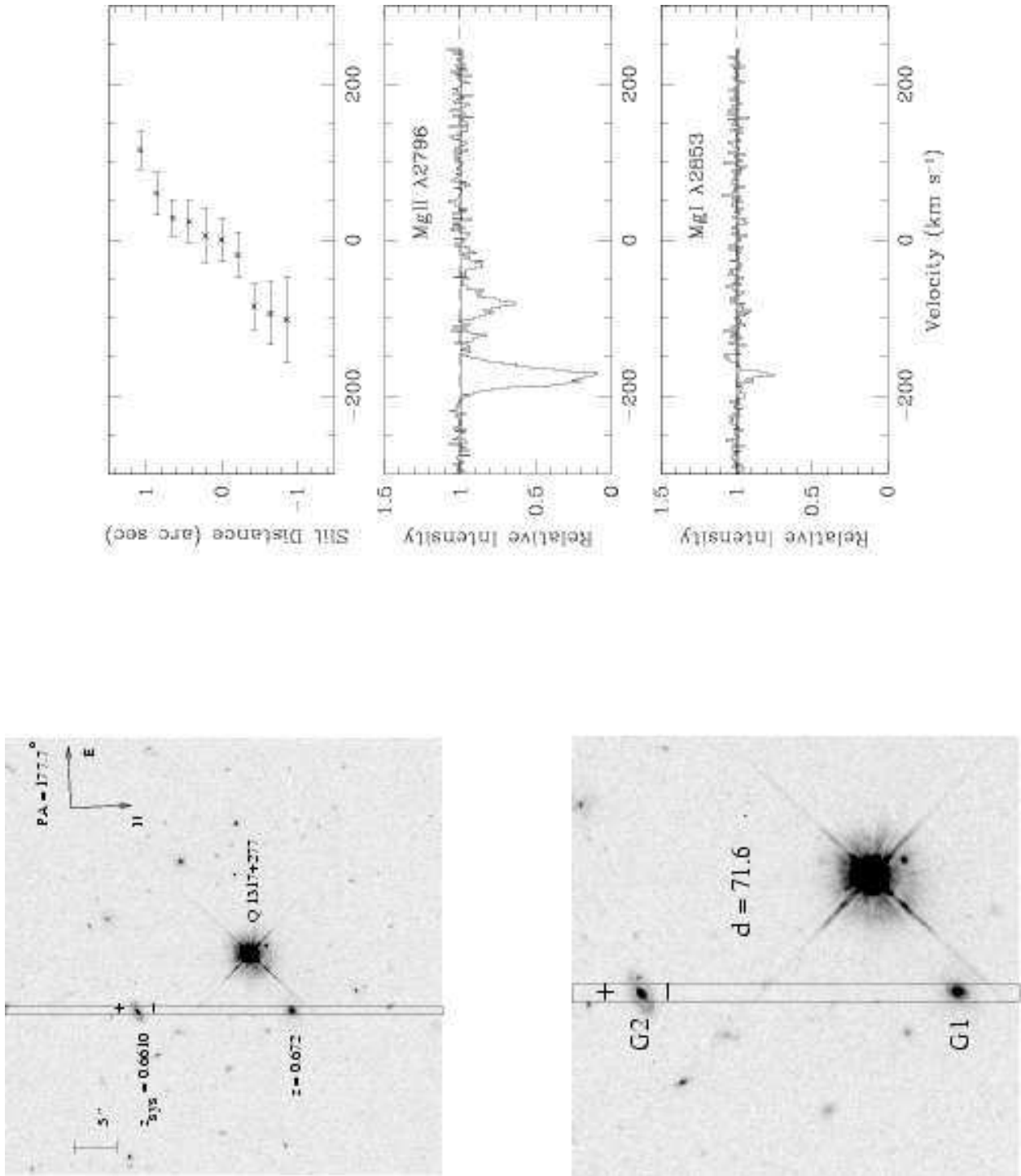


Fig. 5.— a) Same as figure 1, for Q1317+276. b) the observed rotation curve (top) of G2 1317+276, and the kinematics of the Mg II and Mg I absorption (middle, bottom) from the HIRES spectrum of the QSO.

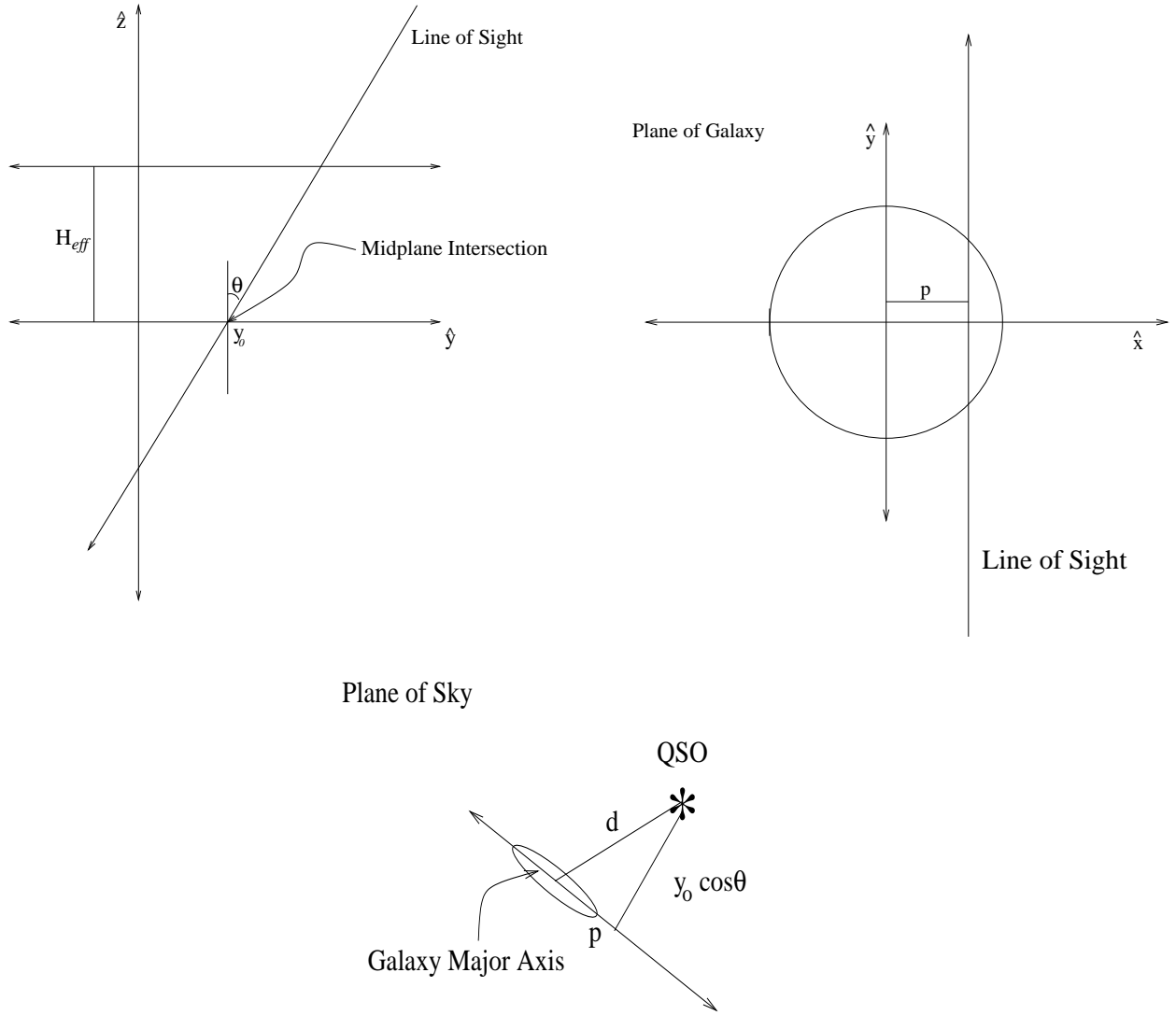


Fig. 6.— Diagrams illustrating the coordinate system used for the kinematic models described in the text. The galaxy disk is located in the  $(x, y)$  plane; the axes are defined such that the line of sight maintains a constant  $x$  distance  $p$  from the  $y$  axis, and the  $y$  axis is parallel to the line of sight.  $H_{\text{eff}}$  is the effective thickness of the disk of material capable of giving rise to detectable Mg II absorption,  $y_0$  is the galaxy  $y$  coordinate where the line of sight intersects the mid-plane.  $d$  is the projected distance of the QSO sightline from the galaxy centroid (as in Figures 1a-5a).

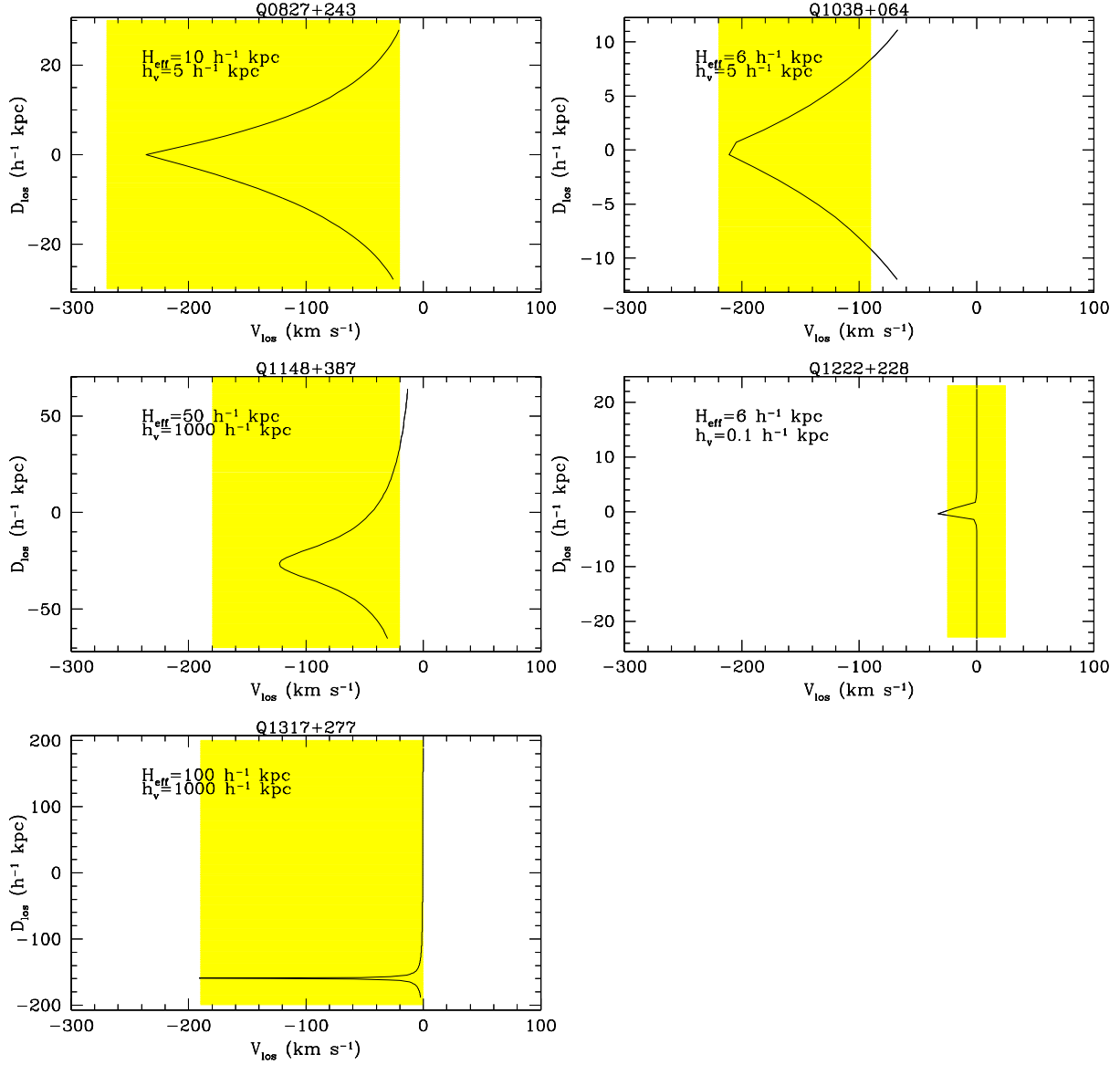


Fig. 7.— Expected velocity as a function of position along the LOS for a) G1 0827+243 b) G1 1038+064 c) G1 1148+387 d) G1 1222+228 and e) G2 1317+276. The model parameters used to generate the velocity curves are summarized in table 5. The distance along the line of sight  $D_{\text{los}}$  is set such that the intersection with an extrapolation of the disk midplane occurs at zero. The range of velocities observed for the Mg II absorption in each case is indicated by the shaded region.